ATMOSPHERIC SCIENCE LETTERS
Atmos. Sci. Let. **12**: 281–287 (2011)
Published online 6 May 2011 in Wiley Online Library
(wileyonlinelibrary.com) **DOI:** 10.1002/asl.334

RMetS
Royal Meteorological Society

Sensitivity of Kelvin waves and Madden–Julian oscillation to convective downdrafts in the NCAR-CAM3

Saroj K. Mishra[1,2]* and Sandeep Sahany[3]

[1]*National Center for Atmospheric Research (NCAR), Boulder, CO, USA*
[2]*Department of Computer Science, University of Colorado, Boulder, CO, USA*
[3]*Department of Atmospheric and Oceanic Sciences, University of California, Los Angeles, CA, USA*

**Correspondence to:*
Saroj K. Mishra, Institute for Mathematics Applied to Geosciences (IMAGe), National Center for Atmospheric Research (NCAR), Boulder, CO, 80305, USA.
E-mail: saroj@ucar.edu

Received: 12 August 2010
Revised: 15 November 2010
Accepted: 28 January 2011

Abstract

Using NCAR-Community Atmosphere Model version 3 (CAM3), the sensitivity of Kelvin waves (KWs) and Madden–Julian Oscillation (MJO) simulation to convective downdrafts is examined. For this, numerical simulations are carried out by changing the downdraft intensity. Increase in the intensity of convective downdrafts in the model leads to greater re-evaporation of precipitation, which enhances the moisture in the lower troposphere, with a corresponding increase in the convective available potential energy (CAPE). Stronger downdrafts, and hence enhanced CAPE, are found to be more favorable for low frequency variability and less favorable for the higher frequencies, leading to stronger MJO and weaker KWs. Copyright © 2011 Royal Meteorological Society

Keywords: global climate model; convective downdrafts; Kelvin waves; Madden-Julian oscillation; tropical meteorology

1. Introduction

The Madden–Julian Oscillation (MJO) and Kelvin waves (KWs) are two dominant modes of variability in the tropical atmosphere. Both are categorized as eastward propagating convectively coupled equatorial waves (CCEWs), but are of different spatial and temporal scales. MJO exhibits planetary spatial scales and time scales of approximately 40 days (Zhang, 2005); KW occurs at synoptic spatial scales with a typical time scale of around a week (Wheeler and Kiladis, 1999). While MJO moves at an average speed of 5 m s^{-1}, KWs generally move at around 10–20 m s^{-1}. In the tropics, deep convection is the primary source of precipitation, which is often organized and influenced by MJO and KWs. These waves significantly affect the tropical weather and climate, and hence are important for both weather and climate predictions. However, poor simulation of these phenomena is a generic problem in most of the current generation circulation models (Lin *et al*., 2006).

Convective parameterization is crucial to the simulation of CCEWs (Maloney and Hartmann, 2001; Mishra, 2007). Convective scale downdrafts are a major component of the convective systems, influencing model simulations significantly (Maloney and Hartmann, 2001; Sahany and Nanjundiah, 2008). From past studies based on observations, it is known that convective downdrafts cool and dry the lower troposphere immediately near the convection zone (Houze, 1977; Tian *et al*., 2006; Yang *et al*., 2008); however, they promote a cooler and moister mean condition in the lower troposphere due to weaker compensating subsidence away from convection (Cheng, 1989). Sahany and Nanjundiah (2008) have demonstrated the impact of convective downdrafts on mean climate in Community Atmosphere Model version 3 (CAM3), by varying the strength of downdrafts in a wide range. They showed that downdrafts make the lower troposphere cooler and moister. The low level moistening in turn enhances the convective available potential energy (CAPE) and reduces the stability of the atmosphere, which is counterintuitive, as downdraft is thought to stabilize the atmosphere. As stability of the atmosphere is one of the important factors influencing the wave propagation (Neelin and Zeng, 2000), it is desirable to understand the impact of downdrafts on the simulation of CCEWs, which is important for simulating tropical intraseasonal variability. These motivate the work, and hence the purpose of the study is to understand the effects of downdrafts on the simulation of MJO and KWs, the two dominant components of tropical intraseasonal variability.

2. Model and experimental details

The numerical model used in this study is CAM3, an atmospheric general circulation model (AGCM) developed by NCAR in collaboration with the atmospheric modeling community. For a detailed description of CAM3, see Collins *et al*. (2004); however, some of the salient components are briefly described below.

For this study, the semi-Lagrangian dynamical (SLD) core was used at 64×128 horizontal resolution with 26 vertical levels. The model uses a hybrid vertical coordinate, which is terrain following at the Earth's surface, but reduces the pressure coordinates at higher levels near the tropopause. The

physical parameterization package consists of moist precipitation processes, clouds and radiation processes, surface processes, and turbulent mixing processes. The moist precipitation processes consist of deep convective, shallow convective, and stratiform components. Deep convection is parameterized using the Zhang and McFarlane (1995) cumulus parameterization scheme.

We carried out three 10-year (January 1979 to December 1988) simulations in atmospheric model intercomparison project (AMIP) framework, by varying the intensity of convective downdrafts. It was varied by changing alpha (α), in the following downdraft formulation (ZM95), with the default value being 0.1:

$$M_d(Z) = ((-\alpha \times M_b) \times (\exp(\lambda_m \times (Z_d - Z)) - 1))/(\lambda_m \times (Z_d - Z)) \quad (1)$$

where, M_d is the downdraft mass flux at any height Z, α is the proportionality factor, M_b is the cloud base mass flux, λ_m is the maximum downdraft entrainment rate, and Z_d is the height of initiation of downdrafts. Note that this function is defined for values of Z less than Z_d. In one experiment α was set to 0, i.e. downdraft is switched off, in second experiment α was set to 0.1 (minimal strength, also the default value), and in the third experiment it was set to 0.7 (strong downdraft).

3. Results

In Figure 1, we show the KWs and MJO in the frequency-wavenumber plane, for both observation and model simulations. To construct this plot, we followed the method of Wheeler and Kiladis (1999) (hereafter WK). Since KWs and MJO are eastward propagating equatorial waves, we have only shown the positive wavenumbers. The figure shows the symmetric component of the normalized power spectra of outgoing longwave radiation (OLR) averaged from 15 °S to 15 °N. This normalization of the power spectra removes a significant fraction of the systematic biases within the models, and gives a clearer picture of the model disturbances with respect to their own climatological variances at individual scales. The regions of wavenumber-frequency space defining the KW and MJO modes are similar to WK (see Figure 6 of WK). The dispersion curves for KWs with equivalent depths of 12, 25, and 50 m are shown. The signals of KWs and MJO are distinctively seen in the observation (Figure 1(a)). In the regime of KWs, observation shows most of the variance centered around an equivalent depth of 50 and 25 m at lower and higher wavenumbers, respectively. This indicates the decrease of phase speed of the waves at smaller scales (see the bending towards 25 m at higher wavenumbers). In the MJO regime, the spectral peaks appear between wavenumbers 1 and 6 and in the period range of 30–70 days, with greater variance at smaller wavenumbers. The variance is predominant at smaller wavenumbers and decreases at smaller spatial scales. This is similar to that seen in the OLR spectra of WK. However, inspection of model results reveals

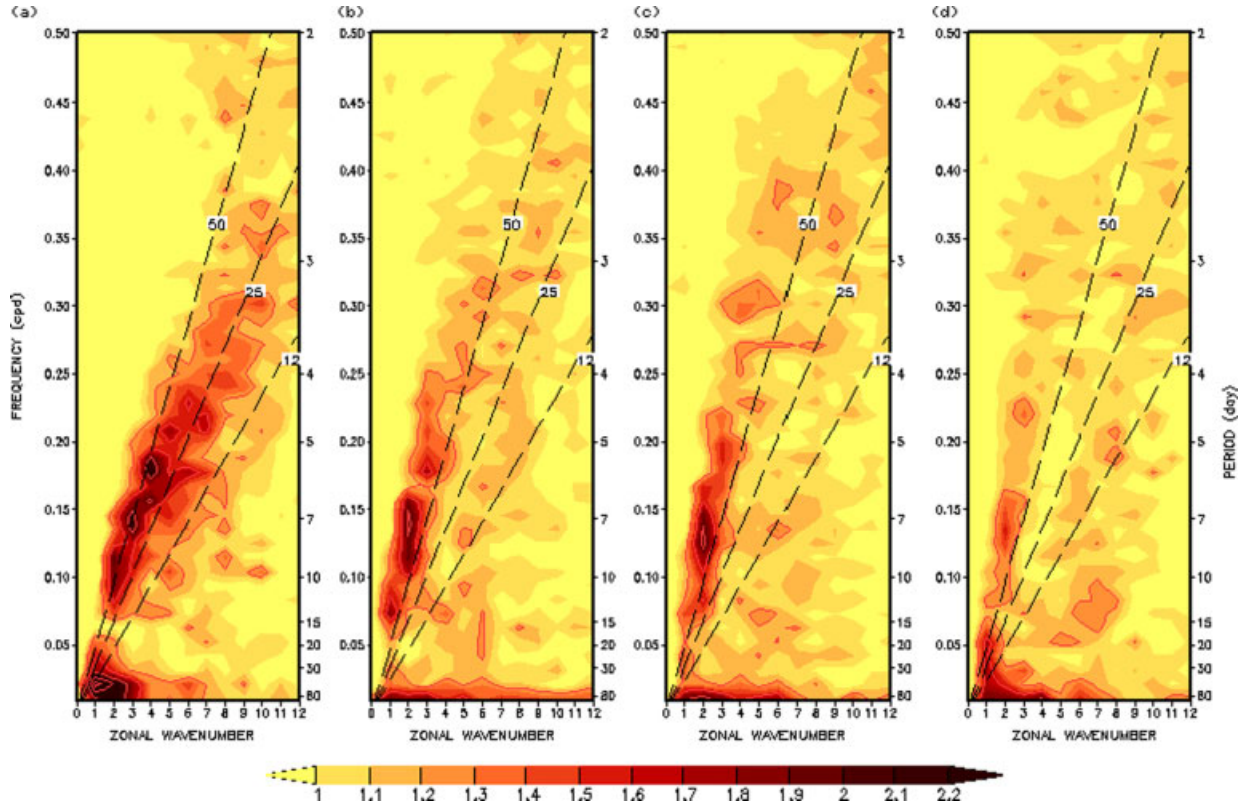

Figure 1. The symmetric-eastward component of the frequency-wavenumber distribution of OLR averaged between 15 °S and 15 °N is shown, (a) AVHRR, (b) NO-DOWNDRAFTS, (c) WEAK-DOWNDRAFTS, and (d) STRONG-DOWNDRAFTS. Wheeler and Kiladis technique is used with 10 years' (January 1979 to December 1988) daily data for this computation.

that there are systematic changes in the KWs and MJO, with change in the intensity of convective downdrafts, specifically, with increase in downdraft intensity, while the KWs become weaker, the MJO becomes stronger. Analysis of the model results with no downdrafts (Figure 1(b)) shows that KWs become more prominent, and move at much higher speeds. The peak in variance is at higher equivalent depths i.e. higher than 50 m for most of the wavenumbers. In the MJO regime, the variance is very weak and distribution is unreasonable. Unlike what is seen in observations, here variance shows up at all wavenumbers with almost similar magnitudes. There is almost no variance at higher frequency bands (below 50 days period) of the MJO regime. When downdraft was incorporated, with a minimal intensity ($\alpha = 0.1$; default value used in the model), KWs do not show any such dramatic change. However, in the MJO regime, there are some notable changes. The variance at larger wavenumbers (above 7) reduces, accompanied with an enhancement at smaller wavenumbers. Secondly, there is a marginal increase in the variance at higher frequency bands of the MJO regime. When downdraft strength was further increased, the changes become more prominent. The KWs become too weak, whereas the MJO becomes more energetic and closer to observations. The variance at higher wavenumbers (above 7) of the MJO regime significantly decreases, accompanied by a significant increase in the variance at smaller wavenumbers. There is an increase in variance in the higher frequency bands of the MJO regime. Thus, the wavenumber-frequency distribution of the simulated MJO becomes more reasonable with strong downdrafts. In order to gain an overall idea about the effects on other CCEWs, i.e. $n = 1$ equatorial Rossby (ER), mixed Rossby-gravity (MRG), $n = 0$ eastward inertio-gravity (EIG), $n = 1$ westward inertio-gravity ($n = 1$ WIG), and $n = 2$ westward inertio-gravity ($n = 2$ WIG) waves, we examined them in wavenumber-frequency domain using the WK methodology. However, we did not notice any such systematic and remarkable change (not shown here), except that EIG and ER become marginally weaker and stronger, respectively, with an increase in downdraft intensity.

Figure 2 shows the magnitude and geographical distribution of variance (unfiltered, 20- to 100-day filtered, and percent accounted for by the 20- to 100-day band relative to unfiltered) of OLR for all seasons from observation, NO-DOWNDRAFTS, WEAK-DOWNDRAFTS and STRONG-DOWNDRAFTS. The filtering is done using a 201-point Lanczos filter that has half power points at 20- and 100-day periods (using the MJO simulation diagnostics, Waliser *et al*., 2009). A close comparison of the

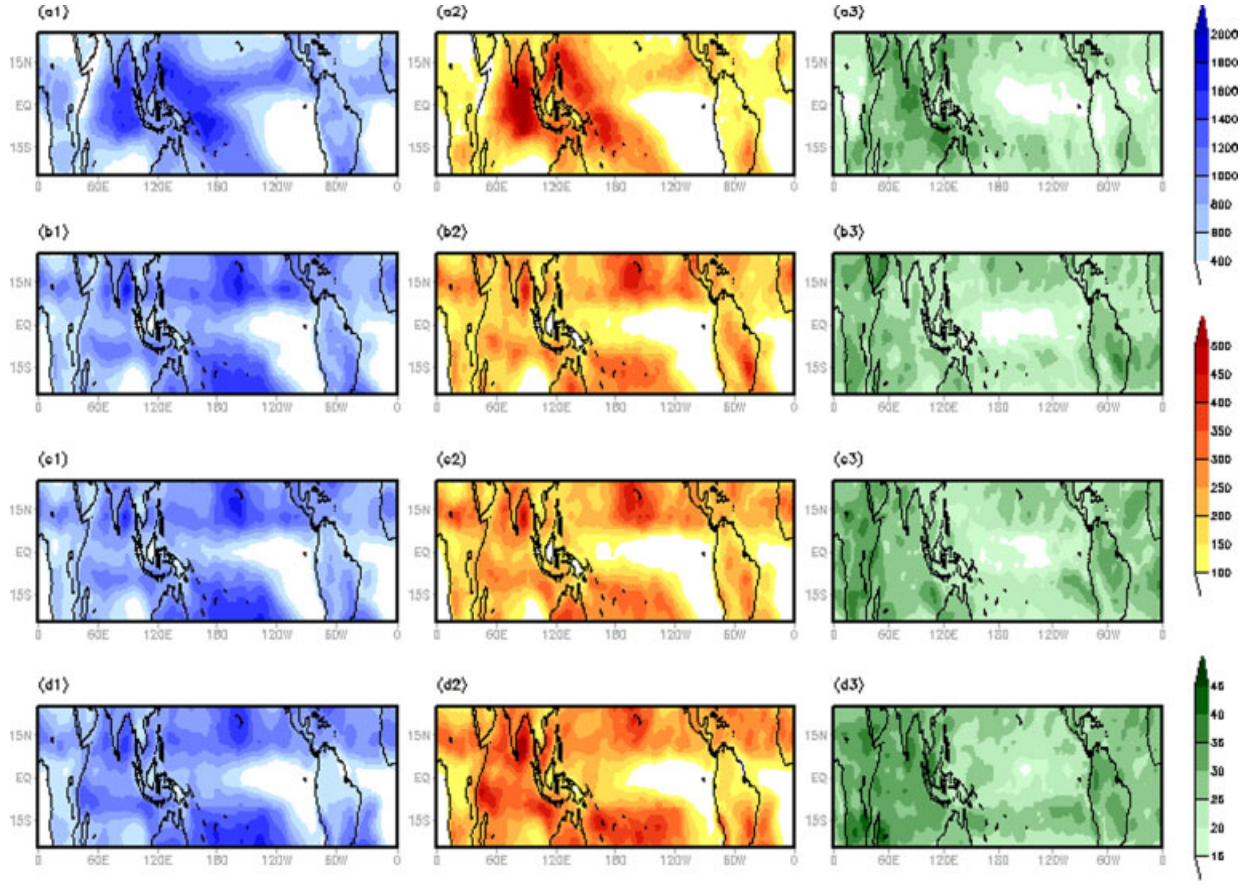

Figure 2. First column of the figure shows unfiltered variance of daily OLR $[Wm^{-2}]^2$ for all seasons: (a1) AVHRR, (b1) NO-DOWNDRAFTS, (c1) WEAK-DOWNDRAFTS, and (d1) STRONG-DOWNDRAFTS. Second column of the figure shows as in first column but for 20- to 100-day filtered variance. In third column, 20- to 100-day filtered variance is expressed as a percentage of unfiltered variance. Daily data for 10 years (January 1979 to December 1988) has been used in this analysis.

maps illustrates that the unfiltered variance is nearly similar in all three simulations, in both spatial pattern and magnitude. However, the 20- to 100-day filtered variance is different: the magnitude increases over the Indian Ocean (IO) and South Pacific Convergence Zone (SPCZ), accompanied by a decrease over northeastern Pacific, and makes it more reasonable. The prominence of the MJO is emphasized by percent variance accounted for by the 20- to 100-day band relative to unfiltered variance (similar to Waliser *et al*., 2009). In observations, the 20- to 100-day variance is predominant in IO, with a magnitude of about 30–40% and about 20% in Western Pacific (WP) and South Pacific (SP). However, in the NO-DOWNDRAFTS case, the above-mentioned features are not realistically represented. With the incorporation of downdrafts, the representation improved and in STRONG-DOWNDRAFTS case, the representation is much similar to what is seen in observations. Nevertheless, some of the shortcomings are still present, for example, the geographical distribution of unfiltered variance is still underestimated over IO and WP; the 20- to 100-day variance over WP is underestimated; the location of the 20- to 100-day variance maximum is not located over the eastern IO as seen in observations. Some of these biases are a known problem with CAM (Sperber, 2004), and other modifications of the convective parameterization have led to improvement in the quality of simulations (Maloney and Hartmann, 2001; Liu *et al*., 2005). We examined the seasonally stratified data for boreal summer and winter separately and noticed similar behavior as discussed in the preceding, i.e. unfiltered variance does not show considerable change; 20- to 100-day filtered variance increases over IO and SPCZ in both the seasons; the 20- to 100-day variance over the north-eastern Pacific decreases in boreal winter. Thus, it can be concluded that the total variance is largely insensitive to downdraft intensity, but the 20- to 100-day variance increases with stronger convective downdrafts. This is consistent with the results seen in wavenumber-frequency domain, i.e. with stronger downdrafts, variance in low frequency regime (MJO and ER modes) increases, while that in the high frequency regime (Kelvin and EIG modes) decreases.

Figure 3 (left column) shows the mean state of OLR from observations and model simulations for all seasons. The mean observed features and that seen in

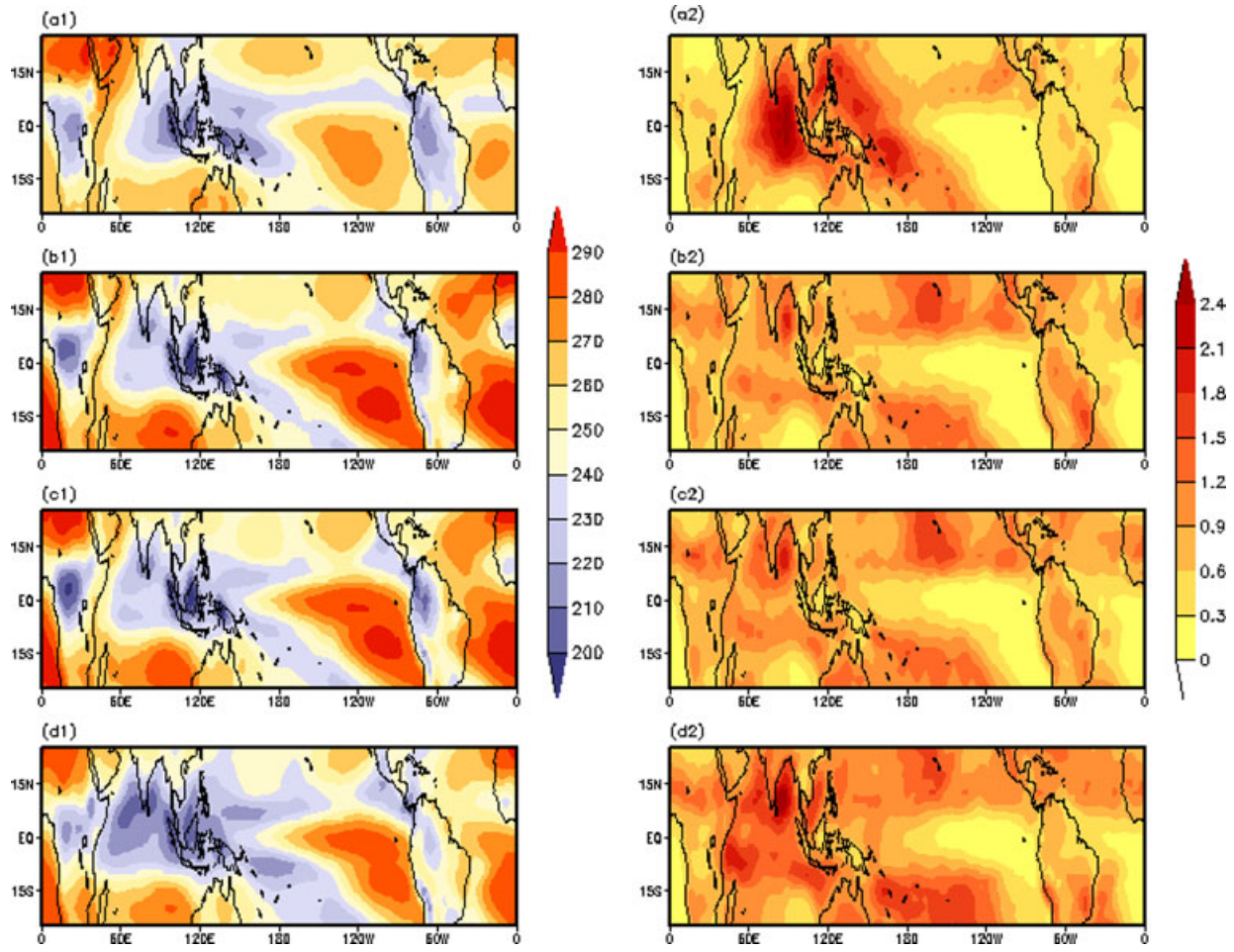

Figure 3. Left column: All season (January 1979 to December 1988) mean of daily OLR [Wm^{-2}] from (a1) AVHRR, (b1) NO-DOWNDRAFTS, (c1) WEAK-DOWNDRAFTS, and (d1) STRONG-DOWNDRAFTS. Right column: Normalized 20- to 100-day variance of daily OLR [$Wm^{-2}]^2$ for all seasons: (a1) AVHRR, (b1) NO-DOWNDRAFTS, (c1) WEAK-DOWNDRAFTS, and (d1) STRONG-DOWNDRAFTS. Normalization is done against their own mean.

the model are similar in many respects: minimum occurs over the maritime continents; low OLR over IO, WP, SPCZ, equatorial Pacific, Central Africa, and South America (due to the presence of deep convection); high OLR over the off-equatorial Pacific and Atlantic Oceans and southern IO (suggesting lack of deep convective clouds). However, the OLR over Central Africa and South America is underestimated and overestimated, respectively. Over eastern Pacific, it is overestimated, and over the Atlantic, it is overestimated. When convective downdrafts were included, some of the above-mentioned biases reduced, e.g. over Africa, eastern Pacific, and the Atlantic. A close comparison of Figures 2 and 3 illustrates that the 20- to 100-day variance over IO, SPCZ, WP, and northeastern Pacific increases with stronger downdrafts, whereas the response of mean OLR is just the reverse. Figure 3 (right column) shows the normalized 20- to 100-day variance of daily OLR. The normalization is done against their own mean. It is seen that the normalized 20- to 100-day variance increases over the IO, SPCZ, and WP, accompanied by a decrease over the northeastern Pacific. This implies that the increase in variance is not due to the increase in the mean value; rather, convective activity over there becomes more pronounced (lower the OLR stronger the convection), and frequency of variations becomes lower (since variance in low frequency modes increases and that in high frequency modes decreases).

Figure 4 shows the mean and standard deviation (SD) of the CAPE, averaged between 15 °S and 15 °N from the three simulations, i.e. NO-DOWNDRAFTS, WEAK-DOWNDRAFTS, and STRONG-DOWNDRAFTS. One of the notable differences is that the inclusion of downdrafts and/or increase in its strength leads to an increase in CAPE over the equatorial belt. In addition, the SD of CAPE (see the gray shading in the figure) increases. Downdraft causes cooling in the lower troposphere by re-evaporating the precipitating rainfall (e.g. Sahany and Mishra, 2011), which acts as a negative feedback for convection. Thus, the SD/variance of convection associated quantities, for example, CAPE and OLR, increases. The increase in mean CAPE with the inclusion of downdraft or increase in its strength indicates an increase in the instability of the atmosphere. This is consistent with the aqua-planet results of Sahany and Nanjundiah (2008). With stronger downdrafts, the re-evaporation

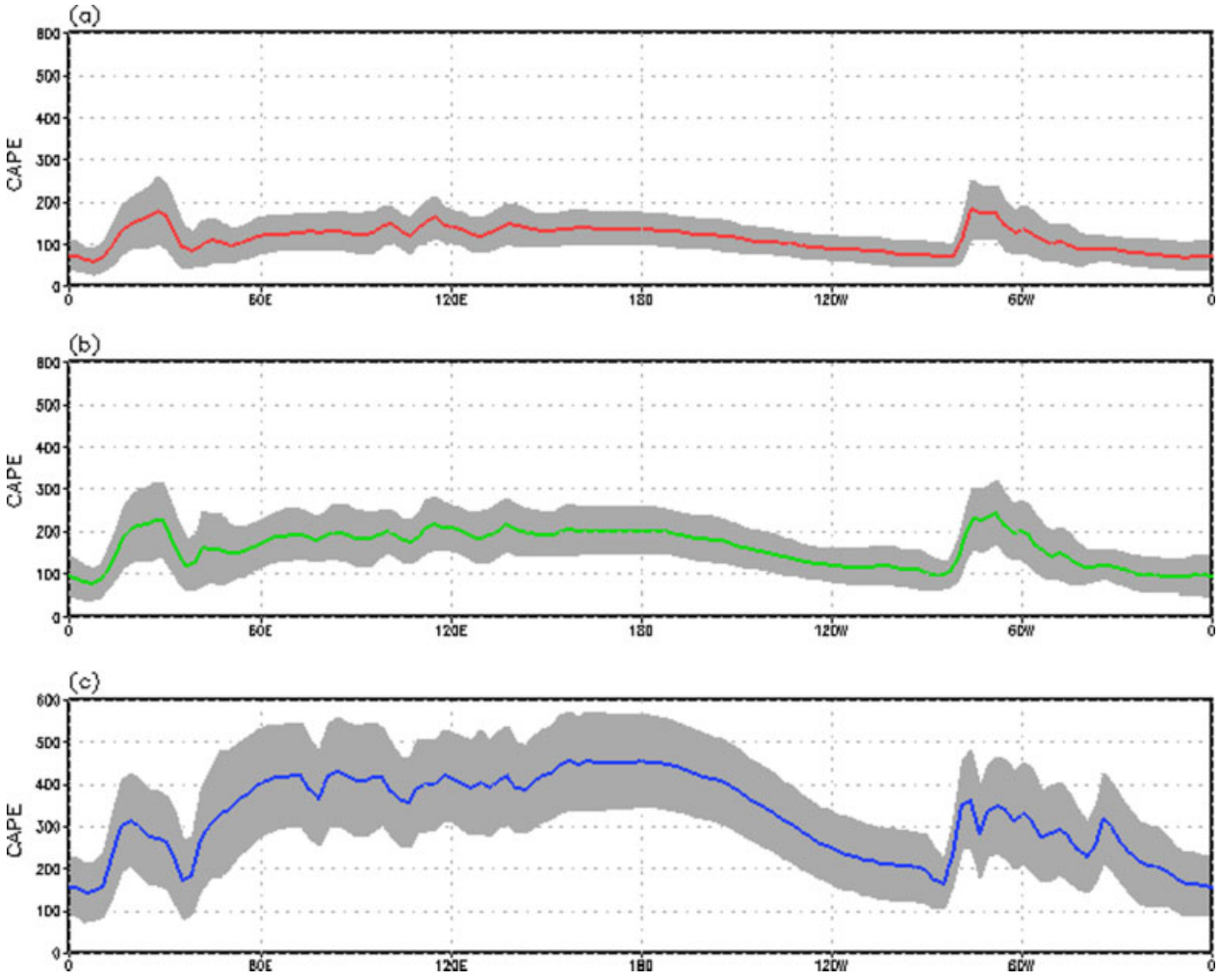

Figure 4. Mean (solid lines) and standard deviation (gray shadings) of CAPE (J.kg^{-1}) averaged between 15 °S and 15 °N from (a) NO-DOWNDRAFTS, (b) WEAK-DOWNDRAFTS, and (c) STRONG-DOWNDRAFTS.

of precipitating rainfall increases the moisture in the lower troposphere of the model (e.g. Sahany and Mishra, 2011). This leads to an increase in CAPE, a measure of the atmospheric instability. Since atmospheric stability controls the wave speeds, i.e. higher the stability, faster is the wave speed (Neelin and Zeng, 2000; Tian and Ramanathan, 2003), with stronger convective downdrafts the low frequency modes (MJO and ER) become pronounced and the high frequency modes (Kelvin and EIG) become weak.

We then examine the variation of precipitation (PRECIP) for the 10-year period spanning January 1979–December 1988, over the regions of prominent MJO activity i.e. eastern IO and WP, using daily data from the three simulations. In Figure 5, the variation of daily PRECIP averaged over a $5° \times 5°$ box over eastern IO (90 °E to 95 °E and 2.5 °S to 2.5 °N) for a representative year (1979) is shown. It is noticed that the seasonal cycle is similar in all the three simulations. However, there is a distinct difference in the frequency of variations. In the NO-DOWNDRAFTS simulation (see top panel), high frequency variations are noticed. The rain events do not last for a long time; rather, they occur at shorter time scales of few days. The temporal variation and its scales are similar to that of the KWs. This indicates the dominance of KWs in the model climate simulated in the NO-DOWNDRAFT case. The lower panels of the figures reveal the change in the frequency of variation with change in the strength of the downdrafts. In STRONG-DOWNDRAFTS simulation, the rain events last for several days and occur at longer time scales. There are distinct active and break phases in time. This indicates the dominance of the MJO in STRONG-DOWNDRAFT simulations. The simulated variability in the WEAK-DOWNDRAFTS case lies somewhere in between the other two cases. This is a manifestation of the decrease in the high frequency variability and increase in low frequency variability with an increase in the strength of downdrafts, which was seen in the frequency-wavenumber plane (Figure 1). Some other years and locations over the region were also examined and similar results were obtained (figure not shown).

4. Discussions and conclusions

This study shows the sensitivity of KWs and the MJO to convective downdrafts in NCAR-CAM3. Three

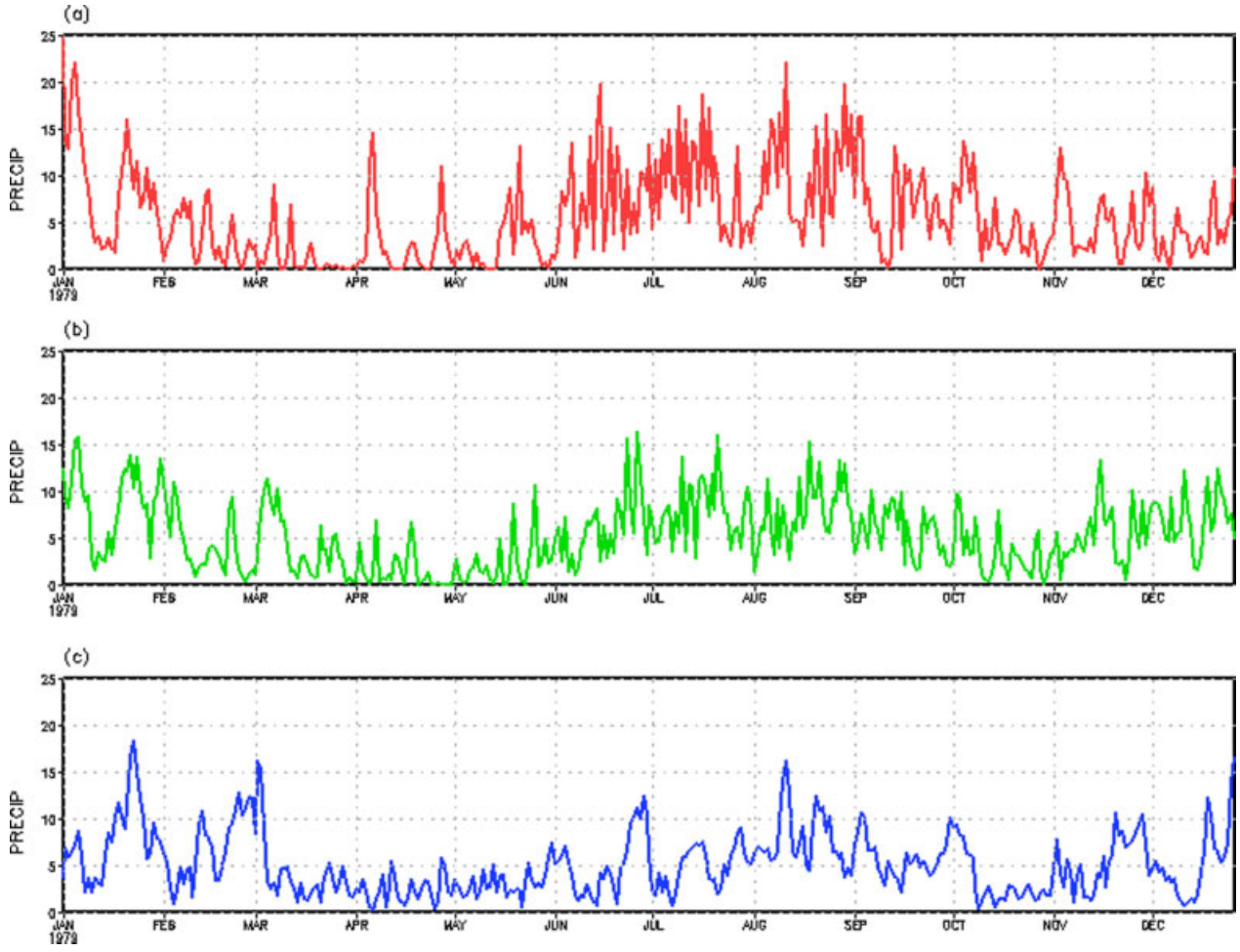

Figure 5. Time series of precipitation (mm day^{-1}) in a box (90 °E to 95 °E and 2.5 °S to 2.5 °N) over the eastern Indian Ocean from NO-DOWNDRAFTS, WEAK-DOWNDRAFTS, and STRONG-DOWNDRAFTS for a representative year. Daily model outputs are used.

simulations were carried out, by varying the strength of downdrafts, one with zero strength, i.e. by switching off convective downdrafts in the convection scheme, second with minimal strength, and third simulation with strong downdraft. Our analysis suggests that the KWs become weaker, and MJO becomes stronger and more realistic, with stronger downdrafts. The variance of OLR decreases in the high frequency modes, accompanied by an increase in the low frequency modes. However, the total variance is largely similar in the three simulations. Enhancement of variance in the low frequency modes primarily occurs over the IO, SPCZ and WP. The mean OLR over these regions is found to be lower with stronger downdrafts, so the enhancement of variance is not because of the mean values, but a change in the temporal distribution. Convective downdrafts act as a negative feedback to convection, thereby increasing its variability. The re-evaporation of precipitation in the downdrafts moistens the lower troposphere in the model. Therefore, increase in the downdraft strength increases the re-evaporation of precipitation, which in turn enhances the moisture in lower troposphere and a subsequent increase in the CAPE. Thus, with stronger convective downdrafts, the model atmosphere becomes unstable, and hence more favorable for low frequency variability (MJO) than higher frequency ones (KWs).

Acknowledgements

We are grateful to Brian Mapes, Joe Tribbia, and David Neelin for helpful discussions on the related topics, which benefited this work. We also greatly acknowledge the constructive comments by two anonymous reviewers and suggestions by the associate editor, Wojciech Grabowski, which helped improve the manuscript. Our appreciation is expressed to editor Alan Gadian for friendly and timely correspondence during the revision.

References

Cheng MD. 1989. Effects of downdrafts and mesoscale convective organization on the heat and moisture budgets of tropical cloud clusters. Part II: effects of convective-scale downdrafts. *Journal of the Atmospheric Sciences* **46**: 1540–1564.

Collins WD, Rasch PJ, Boville BA, Hack JJ, McCaa JR, Williamson DL, Kiehl JT, Briegleb B, Bitz C, Lin SJ, Zhang M, Dai Y. 2004. *Description of the NCAR Community Atmosphere Model (CAM3)*, Tech Rep NCAR/TN-464+STR, National Center for Atmospheric Research: Boulder, CO, 226, pp.

Houze RA Jr. 1977. Structure and dynamics of a tropical squall-line system. *Monthly Weather Review* **105**: 1540–1567.

Lin JL, Kiladis GN, Mapes BE, Weickmann KM, Sperber KR, Lin W, Wheeler MC, Schubert SD, Genio AD, Donner LJ, Emori S, Gueremy JF, Hourdin F, Rasch PJ, Roeckner E, Scinoccao JF. 2006. Tropical intraseasonal variability in 14 IPCC AR4 climate models. Part I: convective signals. *Journal of Climate* **19**: 2665–2690.

Liu P, Wang B, Sperber KR, Li T, Meehl GA. 2005. MJO in the NCAR CAM2 with the Tiedtke convective scheme. *Journal of Climate* **18**: 3007–3020.

Maloney ED, Hartmann DL. 2001. The sensitivity of intraseasonal variability in the NCAR CCM3 to changes in convective parameterization. *Journal of Climate* **14**: 2015–2034.

Mishra SK. 2007. The impact of convective relaxation time on the simulation of seasonal migration of ITCZ, MJO, and Kelvin waves in CAM3.0, *An International Conference: Celebrating the Monsoon*, IISc, Bangalore, http://www.image.ucar.edu/~saroj/presentations.html (Accessed July 2007).

Neelin JD, Zeng N. 2000. A quasi-equilibrium tropical circulation model-formulation. *Journal of the Atmospheric Sciences* **57**: 1741–1766.

Sahany S, Mishra SK. 2011. How do convective downdrafts affect the simulation of rainfall in NCAR-CAM? *Climate Dynamics* (submitted).

Sahany S, Nanjundiah RS. 2008. Impact of convective downdrafts on model simulations: results from aqua-planet integrations. *Annales Geophysicae* **26**: 1877–1887.

Sperber KR. 2004. Madden–Julian variability in NCAR CAM2.0 and CCSM2.0. *Climate Dynamics* **23**: 259–278.

Tian B, Ramanathan V. 2003. A simple moist tropical atmosphere model: role of cloud radiative forcing. *Journal of Climate* **16**: 2086–2092.

Tian B, Waliser DE, Fetzer EJ, Lambrigtsen BH, Yung Y, Wang B. 2006. Vertical moist thermodynamic structure and spatial-temporal evolution of the MJO in AIRS observations. *Journal of the Atmospheric Sciences* **63**: 2462–2485.

Waliser D, Sperber K, Hendon H, Kim D, Maloney E, Wheeler M, Weickmann K, Zhang C, Donner L, Gottschalck J, Higgins W, Kang I, Legler D, Moncrieff M, Schubert S, Stern W, Vitart F, Wang B, Wang W, Woolnough S. 2009. MJO simulation diagnostics. *Journal of Climate* **22**: 3006–3030.

Wheeler M, Kiladis GN. 1999. Convectively coupled equatorial waves: analysis of clouds and temperature in the wavenumber-frequency domain. *Journal of the Atmospheric Sciences* **56**: 374–399.

Yang B, Fu X, Wang B. 2008. Atmosphere-ocean conditions jointly guide convection of the boreal summer intraseasonal oscillation: satellite observations. *Journal of Geophysical Research* **113**(D11): D11105. DOI: 10.1029/2007jd009276.

Zhang C. 2005. Madden–Julian oscillation. *Reviews of Geophysics* **43**: RG2003. DOI: 10.1029/2004RG000158.

Zhang GJ, McFarlane NA. 1995. Sensitivity of climate simulations to the parameterization of cumulus convection in the CCGCM. *Atmosphere-Ocean* **33**: 407–446.

